

8.2 Fringe Localization

Waves traveling through space interfere and produce visible fringes if the conditions are right. In particular, the waves must have some degree of spatial and temporal coherence over a region of space. *Fringe localization* defines the region of space where interference occurs and fringes with reasonably good contrast are observed. There is a wide variety of methods for producing fringes – ranging from a simple parallel plate to complex interferometers, and each has an associated region in space where high-contrast fringes may be observed. The location of this region relative to the components of the interferometer depends on properties of the source and geometry of the interferometer. In this section, basic properties of fringe localization are illustrated for various types of sources and interferometers.

There are several different categories of fringe localization in interferometers. Some of the more common categories are:

- 1) *Localized everywhere*: The fringes have high visibility everywhere in the observation space. (Also called *non-localized* or *unlocalized*.)
- 2) *Localized*: The fringes have high visibility over some surface in the observation space. The fringe localization surface can be curved.
- 3) *Localized at infinity*: A lens is used to transform the angular distribution of fringes into a spatial distribution of fringes on an observation plane with high visibility. The observation plane is usually at the back focus of the lens. Otherwise, fringe visibility is too low for observation. (Also called *Haidinger's fringes* or *fringes of equal inclination*.)
- 4) *Fringes of equal thickness*: Localized fringes, where fringes correspond to contours of constant thickness between two surfaces.

8.2.1 Discussion of sources for illumination

Several types of sources are used for illumination in interferometers and other optical systems. This section discusses basic coherence properties of four different types of sources: monochromatic point source, polychromatic point source, quasi-monochromatic extended source and polychromatic extended source.

8.2.1.1 Monochromatic point source

Any interferometer using an ideal, monochromatic point of light as a source produces high-visibility fringes *everywhere* in observation space. In this case, two-point-source interference produces a hyperboloidal fringe field, as shown in Fig. 8.30. The fringes occur where OPD_0 is an integer number of wavelengths. These fringes are *nonlocalized* or *localized everywhere* or *unlocalized*. Of course, there is no truly ideal monochromatic point source of light. However, a good approximation is found by using high-quality laser sources, where the coherence

length due to the temporal bandwidth of the laser is much greater than the maximum OPD_0 . That is,

$$\frac{c}{n\Delta\nu} \gg (OPD_0)_{\max}, \quad (8.106)$$

where n is the refractive index in observation space.

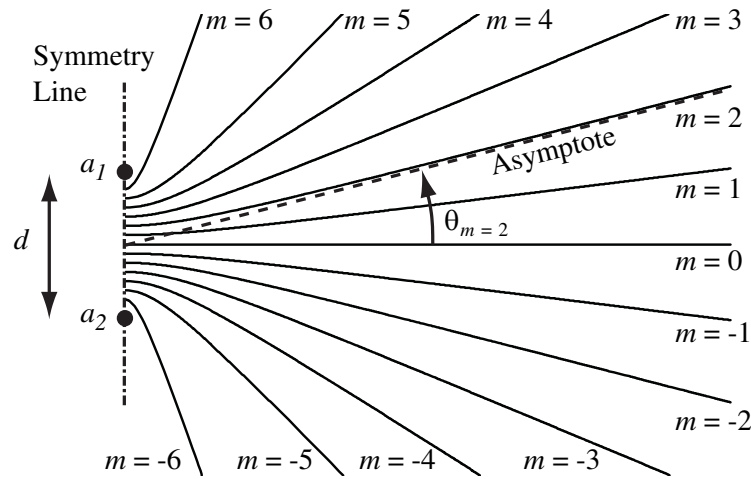


Fig. 8.30. Hyperboloidal fringe field generated from a pair of coherent point sources. Fringe surfaces are hyperboloids of revolution around the symmetry line that passes through both points. The fringe order m increases or decreases away from the plane of zero OPD_0 , which is the $m = 0$ fringe. Asymptotic lines are given by

$$\tan \theta_m = \frac{m\lambda}{\sqrt{d^2 - m^2\lambda^2}}.$$

8.2.1.2 Polychromatic point source

With a polychromatic point emitter in the source space, two-point-source interference produces hyperboloidal fringe fields in observation space for each frequency component of the source's power spectrum. Portions of the fringe field in the observation space with high OPD_0 between the two sources exhibit reduced contrast due to wavelength-dependent fringe variations. Fringe visibility depends on where the observation is made. For example, if $\Delta\nu = c/4\bar{\lambda}$ and $n = 1$, fringe visibility near and beyond the $m = \pm 4$ fringes in Fig. 8.30 would be very poor.

8.2.1.3 Quasimonochromatic extended source

Quasimonochromatic extended sources can be treated as a collection of independent emitters oscillating with wavelength $\bar{\lambda}$.¹ This ideal case might be a good approximation for a highly filtered tungsten lamp or a spectroscopic lamp. The total fringe field in observation space is simply the addition of fringe fields from individual source points. The net effect is usually a decrease in fringe visibility, but the characteristics of the visibility reduction depend greatly on the geometry of the interferometer.

8.2.1.4 Polychromatic extended source

Analysis of systems with a polychromatic extended source must take into account both the temporal bandwidth of the source and its finite extent. In the simplest case, the polychromatic nature can be considered separately. That is, first consider the source as a collection of point emitters at $\bar{\lambda}$, then estimate the additional visibility reduction due to the temporal bandwidth. However, some complicated sources may not be well described in this way. A more complete discussion of this topic is provided in Section 8.3

8.2.2 General procedure for determining fringe localization

There are three basic steps in assessing fringe localization for most interferometers, which are:

- 1) *Determine the fringe period and position in the observation plane given an ideal, monochromatic point source in the source plane;*
- 2) *Integrate fringe patterns resulting from positioning the point source over the spatial extent of the distributed source, and/or from the separate frequencies in the power spectrum; and*
- 3) *Define regions in the observation space where V is large enough ($V > 0.2$) to detect fringes.*

Usually, results from Step (2) produce a relationship that can be expanded into a closed-form solution for fringe visibility in observation space as a function of source properties and interferometer geometry. If a closed-form solution can't be found, a computer simulation can provide the necessary information.

1. In order for the quasimonochromatic assumption to hold over the observation space, Eq. (8.106) must be satisfied.

8.2.3 Application of fringe localization techniques to specific interferometers

In this section, several specific interferometers are analyzed with respect to fringe visibility for different types of sources. The interferometers examined include Young's double pinhole interferometer (YDPI), the plane parallel plate (PPP), a wedged plate, thin films, Fizeau interferometers, the Michelson interferometer, the Twyman-Green interferometer, Lloyd's mirror and Fresnel's biprism.

8.2.3.1 Young's double pinhole interferometer (YDPI)

If a monochromatic point source is used with the YDPI displayed in Fig. 8.1, pinholes produce a coherent pair of source points. The fringes are unlocalized in the entire observation space, which is the entire region to the right of the pinhole plane.

If the YDPI is used with an on-axis polychromatic point source, it produces a region of fringe localization close to the optical axis, as shown in Fig. 8.31, which is specified by Eq. (8.46). The region of fringe localization is bounded by the fringes corresponding to $\pm \text{OPD}_0$ that produce the minimum acceptable visibility V .

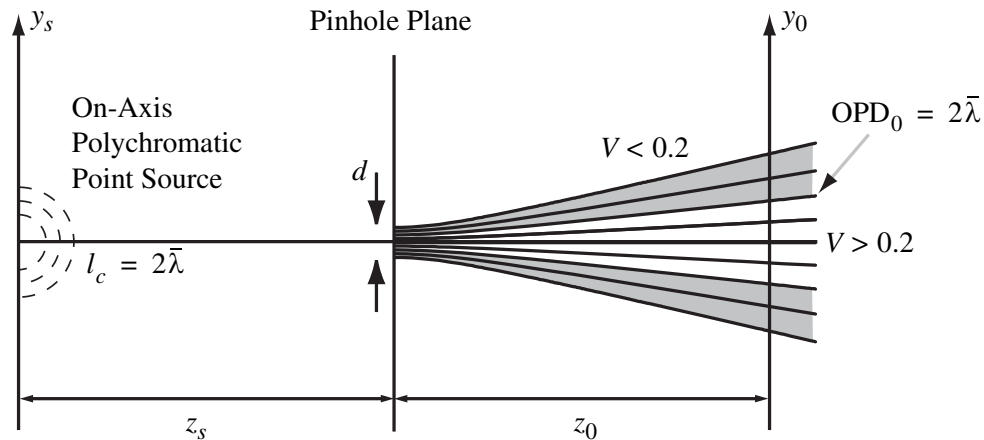


Fig. 8.31. Localization of a YDPI with an on-axis polychromatic point source. A YDPI is used with a polychromatic point source exhibiting a coherence length of $l_c = 2\bar{\lambda}$. Fringes are localized near the axis where $V > 0.2$, which occurs until approximately $\text{OPD}_0 = 2\bar{\lambda}$. The gray region indicates where $V < 0.2$.

Spatial coherence of a YDPI with an extended quasimonochromatic source is examined in detail in Section 8.1.5. Visibility of the fringes in observation space

is a function of the wavelength, the size of the source and its distance to the pinhole plane. Larger sources and smaller distances produce lower visibility. Unlike temporal coherence with the YDPI, visibility due to an extended source is not a function of position in the observation space. Equation (8.79) provides an explicit relationship between the source distribution, interferometer parameters, and visibility.

8.2.3.2 Plane parallel plate (PPP)

The plane parallel plate is shown in Fig. 4.32. If a is a monochromatic point source, fringe visibility is unity everywhere in the observation space to the right of the plate, and the fringes are unlocalized. (For practical experiments, the point source is isolated from the observation region with a beamsplitter or other component.) The glass causes an additional delay between the two waves that must be considered if the source is not monochromatic. Instead of the geometric separation $2t/n$ a delay caused by the maximum $OPD_0 = 2nt$ must be used in the coherence calculations. Therefore, fringes can be observed everywhere in the observation region with good visibility if $2nt \ll c/\Delta\nu$, where t is the thickness of the plate, n is its index of refraction and $\Delta\nu$ is the bandwidth of the source power spectrum. If a is a polychromatic point source with $2nt > c/\Delta\nu$, visibility reduces as the fringe order increases, because of increasing OPD_0 . Fringes of adequate visibility can be observed if the observation plane intersects fringes where $OPD_0 = m\bar{\lambda} < c/\Delta\nu$. Notice that, since the maximum OPD_0 is along the symmetry line, lowest visibility is observed in the center of the fringe pattern.

For a quasimonochromatic extended source, the PPP produces a reflection of each source point for each surface of the plate. A lens can be used to view Haidinger's fringes, as shown by Fig 4.34. Because the fringes are only observed at a sufficiently large distance from the plate, the fringes are said to be *localized at infinity*. Since each fringe results from many source points, but only from a specific angular range, the fringes are also called *fringes of equal inclination*. It is impossible to observe Haidinger's fringes with a white-light source.

8.2.3.3 Wedged plate, thin films, Michelson and Fizeau interferometers

The simplified example of a thin wedge is a very useful demonstration of fringe localization, but it is also useful to develop a general technique to determine fringe localization in other types of interferometers that use quasimonochromatic extended sources including Fizeau, thin film, and Michelson interferometers. A simple construction can be used to determine fringe localization for two-beam interferometers using quasimonochromatic extended sources, as shown in Fig. 8.32. Steps in the construction are:

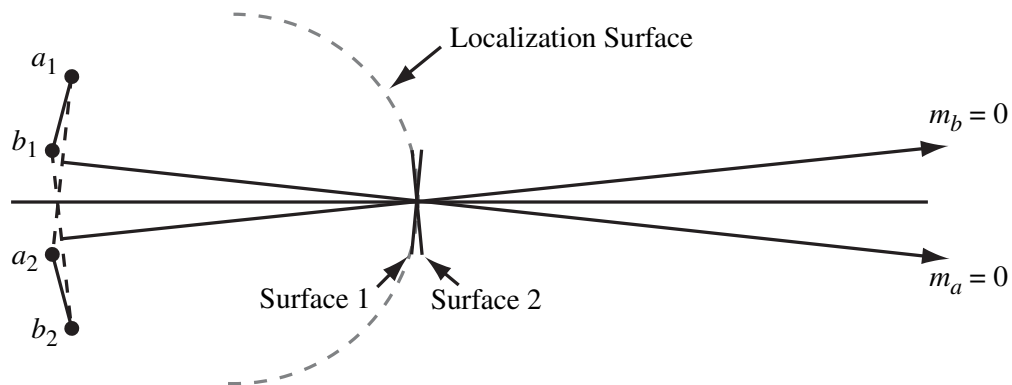


Fig. 8.32. Localization procedure for extended sources. Intersection of $m = 0$ fringes from endpoints of the source images from surfaces of the wedge determines the center of the localization region. Fringes are localized on a curved surface

- 1) Determine positions of the two source images in observation space;
- 2) Locate coherent pairs a_1a_2 and b_1b_2 on ends of the source images;
- 3) Draw symmetry lines between a_1 and a_2 and between b_1 and b_2 ;
- 4) Construct the perpendicular bisectors to each symmetry line. (These bisectors are the $m = 0$ fringes for the coherent pairs.); and
- 5) Find the intersection of the $m = 0$ fringes. This line in space is the center of the localized fringes. The localization surface is a sphere with diameter equal to the distance between the center of the source images and the intersection of the $m = 0$ fringes.

8.2.3.4 Twyman-Green Interferometer

In the Twyman-Green Interferometer displayed in Fig. 4.43, the coherent points are effectively located at infinity. The observation space begins as soon as the beams reflected from each mirror combine. This combination also occurs throughout any optical system that may be used to image the mirrors onto a detector plane. If a point source is used where Eq. (8.106) is satisfied, high visibility fringes are observed throughout the observation region. If a polychromatic point source is used where Eq. (8.106) is not satisfied, the change in visibility versus OPD_0 is given by Eq. (8.46). Since OPD_0 is a function of the mirror separation, visibility can change if the mirrors are moved. A Twyman-Green interferometer is generally not used with extended sources. In that case, the geometry must be analyzed like a Michelson interferometer.

8.2.3.5 Lloyd's mirror

A simple mirror can be used as an interferometer with a polychromatic point source. For example, the Lloyd's mirror interferometer produces a virtual image of the point source, which is located as far below the mirror surface as the real source is above it, as shown in Fig. 8.34. If the total separation is d and the distance between the source plane and the observation plane is z_0 , Eq. 5.46 can be used to predict the region of fringe localization with hyperbolic boundaries. One important difference in the fringe pattern is that the central fringe is dark, instead of bright, if there is a π phase change in reflection off the mirror. Lloyd's mirror with a single point source is similar to the YDPI, in that a hyperboloidal field is generated from two-point-source interference, except for the dark fringe at the center of the field. Straight-line cosine fringes are observed near the optical axis in the observation plane with period $\Lambda = \lambda z_0 / d$.

When the Lloyd's mirror is used with a quasimonochromatic extended source,

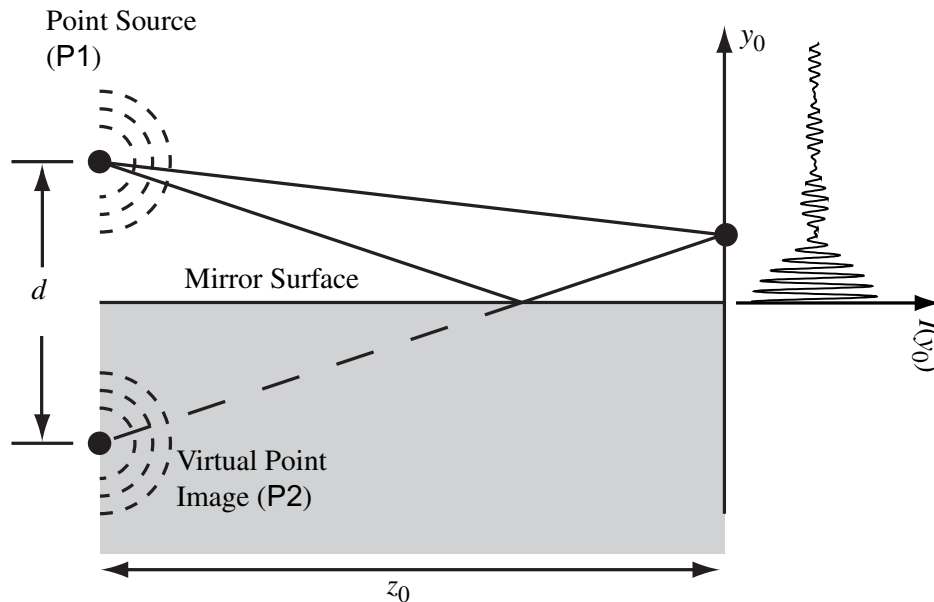


Fig. 8.33. Lloyd's mirror with a polychromatic point source. Fringe visibility is a function of y_0 that depends on the source power spectrum

the distance between individual points and the mirror is not constant, as shown in Fig. 8.35. Therefore, distances between source points and their coherent images are not constant, and the fringe spacing is a function of the source-point position y_s . For simplicity, a perfect mirror is assumed without any loss on reflection. Following a development similar to that used with Eq. (8.80), the integration over the source spatial distribution is

$$\begin{aligned}
I(y_0) &= I_0 \left[2K + 2K \int_{-\infty}^{\infty} \int_{-\infty}^{\infty} m_R(x_s, y_s) \cos(k\text{OPD}_0) dx_s dy_s \right] \\
&= 2KI_0 + 2KI_0 \text{Re} \left\{ \mathbf{F}^{-1} \frac{2y_0}{\lambda z_0} \left[\int_{-\infty}^{\infty} m_R(x_s, y_s) dx_s \right] \right\}, \tag{8.107}
\end{aligned}$$

where K is the fraction of the light emitted by the each source point that reaches the observation plane. If the mean distance from the source distribution to the mirror is \bar{y}_s , an argument similar to that used for Eqs. (8.74) through (8.81) results in

$$\begin{aligned}
I(y_0) &= 2KI_0 + 2KI_0 \left| \mathbf{F}^{-1} \frac{2y_0}{\lambda z_0} \left[\int_{-\infty}^{\infty} f_R(x_s, y_s) dx_s \right] \right| \cos \left[2\pi y_0 \frac{2\bar{y}_s}{\lambda z_0} + \beta(y_0) \right], \\
&= 2KI_L + 2KI_L \mu(y_0) \cos \left[2\pi y_0 \frac{2\bar{y}_s}{\lambda z_0} + \beta(y_0) \right], \tag{8.108}
\end{aligned}$$

where

$$f_R(y_s) = m_R(x_s, y_s - \bar{y}_s), \tag{8.109}$$

$$\mu(y_0) = \left| \mathbf{F}^{-1} \frac{2y_0}{\lambda z_0} \left[\int_{-\infty}^{\infty} f_R(x_s, y_s) dx_s \right] \right|, \tag{8.110}$$

and

$$\beta(y_0) = \arg \left\{ \mathbf{F}^{-1} \frac{2y_0}{\lambda z_0} \left[\int_{-\infty}^{\infty} f_R(x_s, y_s) dx_s \right] \right\} \tag{8.111}$$

Notice that visibility is equal to $\mu(y_0)$, which is a function of the observation-space coordinates. This behavior is dramatically different than the result obtained when an extended quasimonochromatic source is used with a YDPI, where the visibility is constant through the observation space. In fact, with a rectangular source distribution, Lloyd's mirror fringes may appear more like those shown in Fig. 8.2(C).

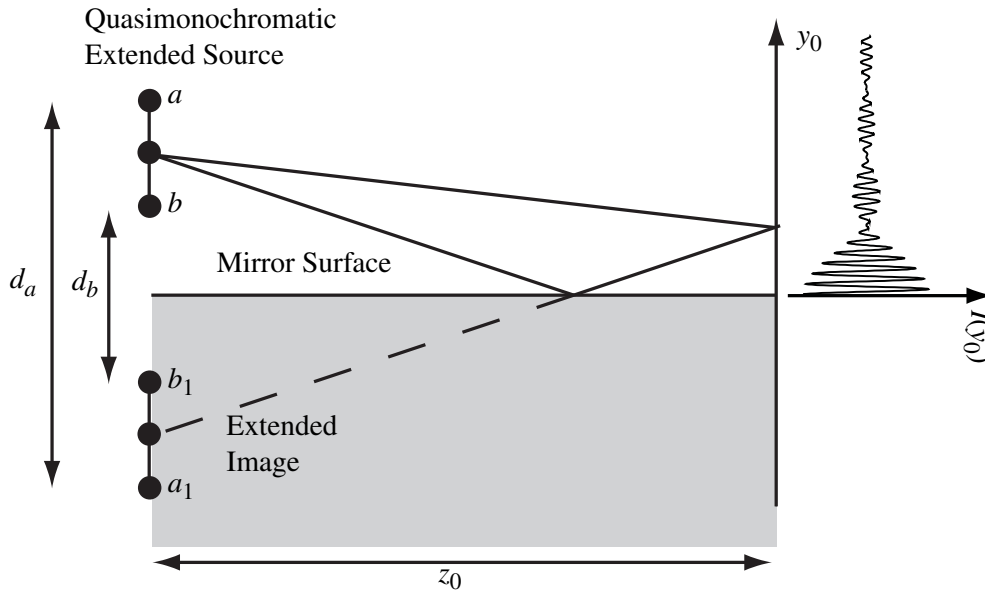


Fig. 8.34. Lloyd's mirror with an extended quasimonochromatic source. Because different positions on the source produce different separations of the source images, the fringe visibility varies as a function of y_0 .

8.2.3.6 Fresnel's biprism

Yet another variation is Fresnel's biprism, as shown in Fig. 8.35 with a polychromatic point source, where two virtual point images a_1 and a_2 are produced by an offset pair of prisms with refractive index n . If the reflections from the prism faces are negligible, then the two virtual point images, one from each prism, produce an interference pattern in much the same way as the YDPI. Analogous to Fig 8.3, distance z_0 is measured from the virtual source plane, which is a distance nl behind the prisms.

Fresnel's biprism with an extended quasimonochromatic source is similar to Lloyd's mirror, except that two virtual images of the source are formed, and the parities of the images are not reversed, as shown in Fig 8.36. That is, the virtual sources are in the same orientation with respect to the y axis, where a_1b_1 and a_2b_2 are upright. (In the Lloyd's mirror, ab interferes with the reversed b_1a_1 .) In Fresnel's biprism, the distance d is a constant between coherent pairs, and the fringe spacing from coherent pairs is not a function of the source-point position. However, the offset in source-pair position produces an offset in the fringe position, which is similar to the YDPI with an extended, quasimonochromatic source. The fringe contrast for Fresnel's biprism is not a function of the observation-space position y_0 , but it is a function of z_0 , λ and d . The net result of applying the procedure listed in Section 8.2.2 is that the visibility of the fringes is found from the coherence factor calculated from Eq. (8.76), where d is the spacing

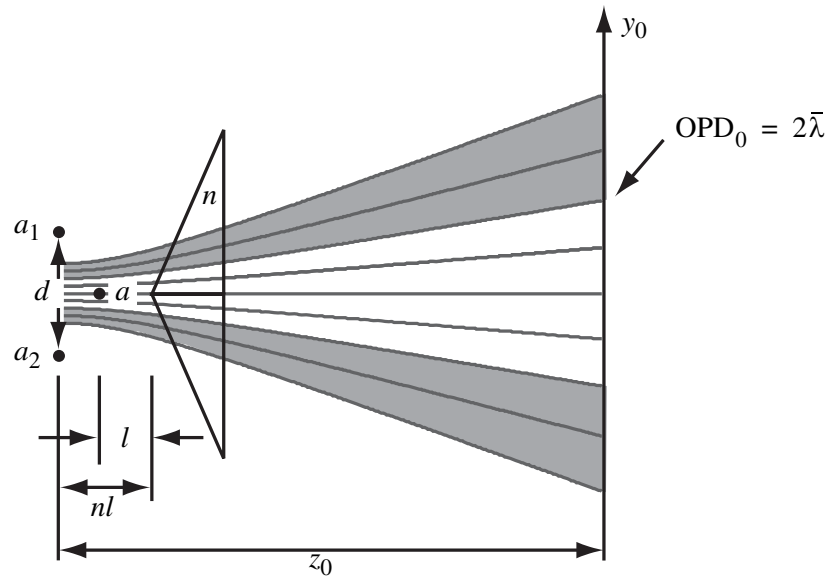


Fig. 8.35. Fresnel's biprism with a polychromatic point source. between coherent pairs and z_0 is the distance between the source images and the observation plane.

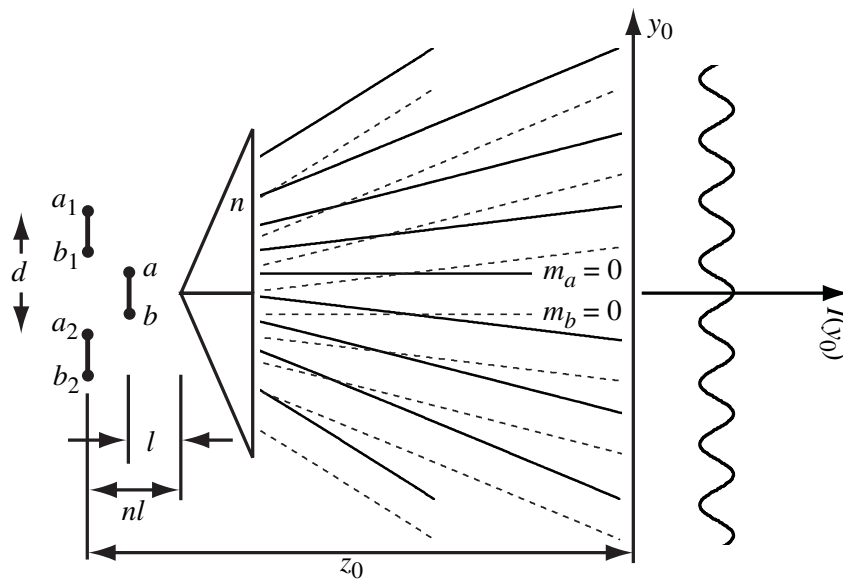


Fig. 8.36. Fresnel's biprism with an extended quasimonochromatic source. Since the parity of the source images is not reversed, fringes formed from coherent pairs have the same period, but different offsets. A uniform reduction in fringe visibility is observed in the observation space.